Synthesis of vanadium oxides 5 wt.%VO$_2$–M$_x$O$_y$ by sol–gel process and application in cyclohexene epoxidation

S EL-KORSO, I REKKAB, A CHOUKCHOU-BRAHAM[*]**, S BEDRANE, L PIRAULT-ROY**[†] **and C KAPPENSTEIN**[†]

Laboratoire de catalyse et synthèse en chimie organique. Faculté des sciences, Université A. Belkaid,
B.P. 119 Tlemcen 1300, Algérie
[†]LACCO UMR 6503, Laboratoire de catalyse, Faculté des sciences Fondamentales et appliquées,
86022 Poitiers Cedex, France

Abstract. A series of SiO$_2$, Al$_2$O$_3$ and TiO$_2$ mixed vanadium materials have been prepared from inorganic precursors via the sol–gel process and subsequently dried, calcined and reduced at elevated temperatures. Structural characterization of these materials was carried out by X-ray diffraction (XRD), N$_2$ adsorption at 77 K, thermal analysis (TGA/DTA), UV-vis diffused reflectance spectroscopy (DR UV-vis) and scanning electron microscopy (SEM) with energy dispersive X-ray (EDX). Their catalytic activities in the epoxidation of cyclohexene with TBHP as oxidant were also examined. Results of XRD and DR UV-visible diffused revealed that VO$_2$ species are predominant in all samples and no formation of V$_2$O$_5$ was detected. Experimental results indicated that the VO$_2$–SiO$_2$ catalysts performed excellently for the epoxidation of cyclohexene by tertiobutyl hydroperoxide.

Keywords. Vanadium oxide; sol–gel; epoxidation; cyclohexene; TBHP.

1. Introduction

The preparation of micro- and mesoporous solids with a high effective surface area has attracted considerable attention because of the potential size-selective properties of such porous materials as catalysts, catalyst supports and filters (Thomas and Thomas 1997; Farrusseng *et al* 2001). The sol–gel technique is an attractive approach for preparing micro/mesoporous oxide materials as powders with high purity and homogeneity due to its flexibility and low temperature preparation of sols and gels (Brinker and Schere 1990). Actually, the ability of sol–gel to form mixed M–O–M′ bonds (where M and M′ denote two different metal atoms) leads to high densities of acid sites, while providing high surface area and pore volume desired for catalytic applications (Miller and Ko 1997). Vanadium is a very special metal with unique mechanical properties. Besides, it is the most important metal used in metal oxide catalysis (Ertl *et al* 1997; Hagen 1999). The oxidation states of the vanadium atoms vary from two to five, and this fact is responsible for its use as a catalyst because of an easy conversion between oxides of different stoichiometries. The principal vanadium oxides are V$_2$O$_5$, VO$_2$, V$_2$O$_3$, VO, and the oxidation state of these oxides decreases from

V$^+$ to II$^+$, respectively. Due to the restrictions of thermal stability, mechanical strength and surface area of vanadium oxides, they are generally not used directly as a catalyst in industry (Weckhuysen and Keller 2003). Microporous molecular sieves incorporated with vanadium were found to be active catalysts for various oxidation reactions (Whitting and Anderson 1993). However, activity and selectivity of these materials are sensitive to the preparation methods (Sen *et al* 1996).

Epoxidation reactions are indispensable for the chemical industry because of the ease with which they can be used to convert olefins to oxygenated molecules, so-called epoxides, by oxygen transfer reaction. Epoxides are valuable and versatile commercial intermediates used as key raw materials for a wide variety of products owing to the numerous reactions they may undergo (Sreethawong *et al* 2005). Cyclohexene epoxidation that yields the cyclohexene oxide is one of the most difficult cases, in which the first two problems, viz. allylic oxidation and epoxide ring-opening, occur considerably. Cyclohexene oxide is an important organic intermediate consumed in the production of pharmaceuticals, plant-protection agents, pesticides and stabilizers for chlorinated hydrocarbons (Technical Data Sheet 1997). Much effort has been dedicated to the development of new active and selective cyclohexene epoxidation catalysts that circumvent the side reactions and subsequent formation of large amounts of by-products (Sreethawong *et al* 2005).

---

[*]Author for correspondence (cba@mail.univ-tlemcen.dz)

The aim of the present study is to provide and to optimize vanadium heterogenous catalyst suitable for cyclohexene epoxidation. This includes the preparation of mixed oxides with 5 wt.% vanadium loading by sol–gel method. BET, XDR, SEM, ATG and UV-Vis DRS spectroscopic techniques are used to study the change of solid structure and vanadium oxidation state on various oxides and investigate the catalytic performance of the prepared catalysts in the selective epoxidation of cyclohexene, in liquid phase, with TBHP as oxidant.

2. Experimental

2.1 *Starting materials*

The following chemicals were employed for the preparation and in catalytic test of 5 wt.%VO_2–SiO_2, Al_2O_3 and TiO_2: tetraethylorthosilicate ($C_8H_{20}O_4Si$, Aldrich 98%), aluminium tributoxide (($C_4H_9O)_3Al$, Aldrich 95%), titane tetraisopropanolate ($Ti(O(CH_2)_3\ CH_3)_4$, Aldrich 97%), ammonium metavanadate (NH_4VO_3; Strem chemicals, 99%), chloridic acid, ethanol, propanol (from Aldrich), cyclohexene (Aldrich 99%), tertiobutyl hydroperoxide (TBHP, Aldrich 70%) and heptane (Fluka 99%).

2.2 *Synthesis*

2.2a *Synthesis of 5 wt.% VO_2–SiO_2 and 5 wt.% VO_2–TiO_2*: The mixed oxide was prepared by an acid-catalyzed sol–gel process (Klein *et al* 1996). A quantity of 0·46 g of ammonium metavanadate (NH_4VO_3) was dissolved in a mixture of 14 mL of titane tetraisopropanolate or 16·22 mL of silicate orthotetraethyl and 13 mL of ethanol or 11·2 mL of propanol. The mixture was stirred for 24 h, and then 4·5 mL of HCl was added to this solution. The resulting solution was stirred for 24 h. This solution was first dried at 333 K for one night, next at 393 K for another night and then calcined at 673 K for 4 h in air and finally reduced to 673 K for 4 h under hydrogen flow. The sample thus obtained was heated at 1073 K for 4 h under an argon flow (28 mL/min).

2.2b *Synthesis of 5 wt.% VO_2–Al_2O_3*: This sample was obtained following the procedure described by Yoldas (1975). The hydrolysis and peptization of 0·11 g of aluminium tributoxide Al ($OC_4H_9)_3$ was carried out by the single addition of 66·6 mL of water at 333 K, under stirring, for 1 h. The addition of 0·11 mL of HCl and 0·57 g of NH_4VO_3 with a temperature increase to 353 K, while stirring for 2 h, lead to gel formation. The gel was dried in an oven, under air flow, at 393 K during one night and finally calcined at 673 K for 4 h in air then reduced at 673 K for 4 h under hydrogen flow. The sample thus obtained was heated at 1073 K for 4 h under an argon flow (28 mL/min).

2.3 *Catalyst characterization*

The VO_2–SiO_2, Al_2O_3 and TiO_2 catalysts have been characterized by X-ray powder diffraction (XRD) using a Bruker D5005 diffractometer with Cu Kα radiation ($\lambda = 1·54060$) in the range of $2\theta = 10$–$80°$ with a step of 0·02° and an acquisition time of 1s.

BET surface area was determined from N_2 adsorption isotherms at 77 K using a Micromeritics Tristar instrument. Prior to the absorption measurements, the sample was degassed at 673 K for 4 h under a flow of 30% nitrogen in helium. Nitrogen physisorption isotherms were analysed using BJH and BET methods.

The prepared samples were analysed by thermal analysis (TGA/DTA) using a device type SDT Q600 instrument. The 20–30 mg sample mass was then introduced into a platinum crucible, which was supported by the beam of a balance in the oven. The analysis was performed in air at a temperature ramp of 5 °C/min in the range 298–1473 K.

These analyses were carried out in the Laboratory of Catalysis in Organic Chemistry (LACCO, UMR6503) Poitiers University, France.

The UV-visible spectra (200–800 nm) of these samples were carried out on UV/Vis spectrometer Perkin Elmer with a Cary 4/5 diffuse reflection sphere. The baseline was recorded using MgO as reference.

Scanning electron microscopy (SEM) with energy dispersive X-ray (EDX) analysis was performed using a Hitachi-TM.1000 at 150 kV acceleration voltage.

2.4 *Catalytic experiments*

The catalytic epoxidation of cyclohexene with tertiobutylhydroperoxide (TBHP) (Aldrich, 70 wt.% in H_2O) as an oxidant, was carried out in a two neck glass round-bottom flask equipped with a magnetic stirrer and a reflux condenser. First, TBHP was stirred with heptanes as solvent in order to perform a phase transfer from water to organic phase. Typically, 25 mL of heptane and 38·45 mmol (5·5 mL) of oxidant (TBHP) were mixed in a closed Erlenmeyer flask and magnetically stirred for 24 h. The organic phase was then separated from the aqueous phase. To control the phase transfer, concentration of the remaining TBHP in the aqueous phase was determined by iodometric titration. Less than 10 % of the initial TBHP remained in the aqueous phase. Then, 29 mmol (3 mL) of cyclohexene was added to the TBHP–heptane mixture. The mixture was heated to 338 K under vigorous stirring, and then the catalyst (100 mg) was added (time zero). The reaction products were identified by comparison with authentic products and the course of reactions was followed by gas chromatography (GC), using a SCHIMADZU 14-B gas chromatograph equipped with a Agile HP–FFAP capillary column. A flame ionization detector (FID) was used and 0·5μL of the sample was analysed. Before GC analysis, remaining TBHP was decomposed by introducing an excess of triphenylphosphine (Aldrich). On the other hand, to

control the remaining TBHP, an iodometric titration was performed at the end of the reaction (after 6 h) by analysing the organic phase.

$$\text{Conversion (\%) = (moles of initial substrate}$$
$$- \text{moles of residual substrate/}$$
$$\text{moles of initial substrate)} \times 100,$$

$$\text{Selectivity (\%) = (moles of individual product/}$$
$$\text{moles of total products)} \times 100.$$

3. Results and discussion

3.1 *Catalyst characterization*

All diffractograms of the prepared catalysts are shown in figure 1. XRD patterns of VO₂–SiO₂ catalysts show a peak at about $2\theta = 22°$, which is broadened due to the partially amorphous nature of silica. The same results have been obtained by Yejun and Can (2007) and Aboelfetoh and Pietschnig (2009). The diffractograms of VO₂–Al₂O₃ calcined and reduced at 673 K show only the characteristic peaks of the Al₂O₃ with boehmite phase (AlO(OH)ₙH₂O) [ICDD pattern 21-307] (Nguefack *et al* 2003). For the sample heated at 1073 K, besides the typical peaks of δ-Al₂O₃ well-defined peaks at $2\theta = 35.2°$, $21.5°$, $25.5°$ and $43°$ [ICDD pattern 46-1215] and corundum ($2\theta = 36°$, $44°$ and $58°$) [ICDD pattern 46-1212] appeared, and $2\theta = 25°$, $32°$, $56°$ and $70°$ correspond to crystalline VO₂ [ICDD pattern 76-0676] (Nguefack *et al* 2003; Aboelfetoh and Pietschnig 2009). The presence of TiO₂ anatase at $2\theta = 25.3°$, $37.8°$, $48.1°$, $55°$, $62.8°$ and $68.9°$ [ICDD pattern 21-1272] was detected as the only crystalline phase of VO₂–TiO₂ (Jiang and Chen 2004; Habel *et al* 2006). XRD analysis does not present any characteristic diffraction peak of VO₂ or other vanadium oxide. Therefore, vanadium oxide will be either amorphous or very well dispersed in the TiO₂ phase (Bellifa *et al* 2006).

The textural properties of catalysts measured by N₂ adsorption according to BET method are summarized in table 1. BET surface areas of the VO₂–SiO₂ was found to decrease from 390 m²/g at 673 K to 5 m²/g at 1073 K just like the BET surface area of VO₂–Al₂O₃ which was found to decrease from 368 m²/g at 673 K to 2 m²/g at 1073 K, due to sintering of the sample at higher calcination temperatures (Reddy *et al* 2006). A progressive decrease in the surface area with increasing calcination temperatures is mainly due to sintering of the sample at higher calcination temperatures, and this is a normal phenomenon (Bond and Tahir 1991; Deo *et al* 1994; Reddy *et al* 2002, 2003). For the same vanadium loading, VO₂–SiO₂ samples develop, in general, in higher surface areas than VO₂–Al₂O₃ samples. However, the latter have larger average pore diameters, which is of interest because of the easy diffusion of reactants into the active sites (Moussa *et al* 2006). The surface of VO₂–TiO₂ (140 m²/g) is lower compared to that of silica and alumina which are respectively, 390 and 368 m²/g due to the grafting of vanadium species in the pores of titanium (Yejun and Can 2007). Nitrogen adsorption–desorption isotherms of samples are shown in figure 2, respectively. The obtained isotherms of VO₂–Al₂O₃ and VO₂–TiO₂ (673 K) can be classified as type-IV, according to the IUPAC (Gregg and Sing 1982; Sing *et al* 1985), associated to the capillary condensation in the

Table 1. BET surface area results for different samples.

Material	Treatment temperature (K)	SBET (m²/g)	Pore volume (cm³/g)	Pore size (Å)
5% VO₂–SiO₂	673	390	0·19	20
5% VO₂–SiO₂	1073	5	0·0002	–
5% VO₂–Al₂O₃	673	368	0·37	40
5% VO₂–Al₂O₃	1073	2	0·0068	196
5% VO₂–TiO₂	673	140	0·12	35
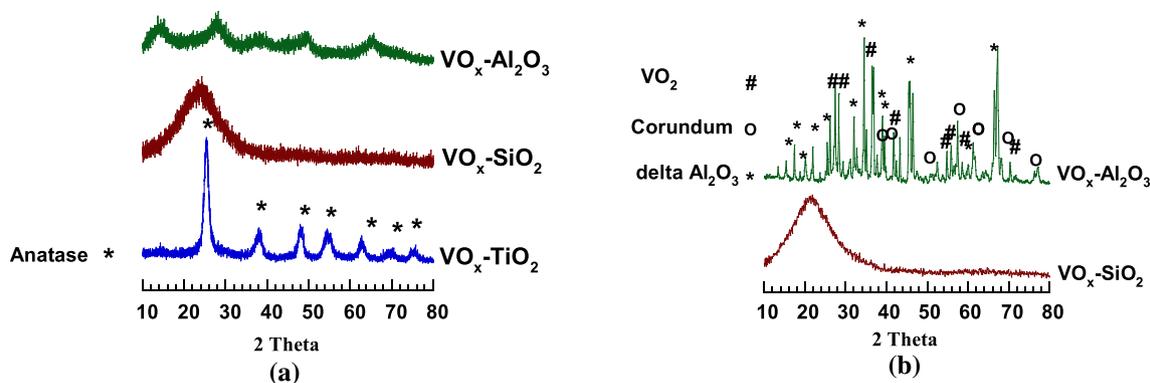
Figure 1. Powder-XRD patterns of 5%VO₂–MₓOᵧ materials; (**a**) calcined–reduced at 673 K and (**b**) heated at 1073 K.
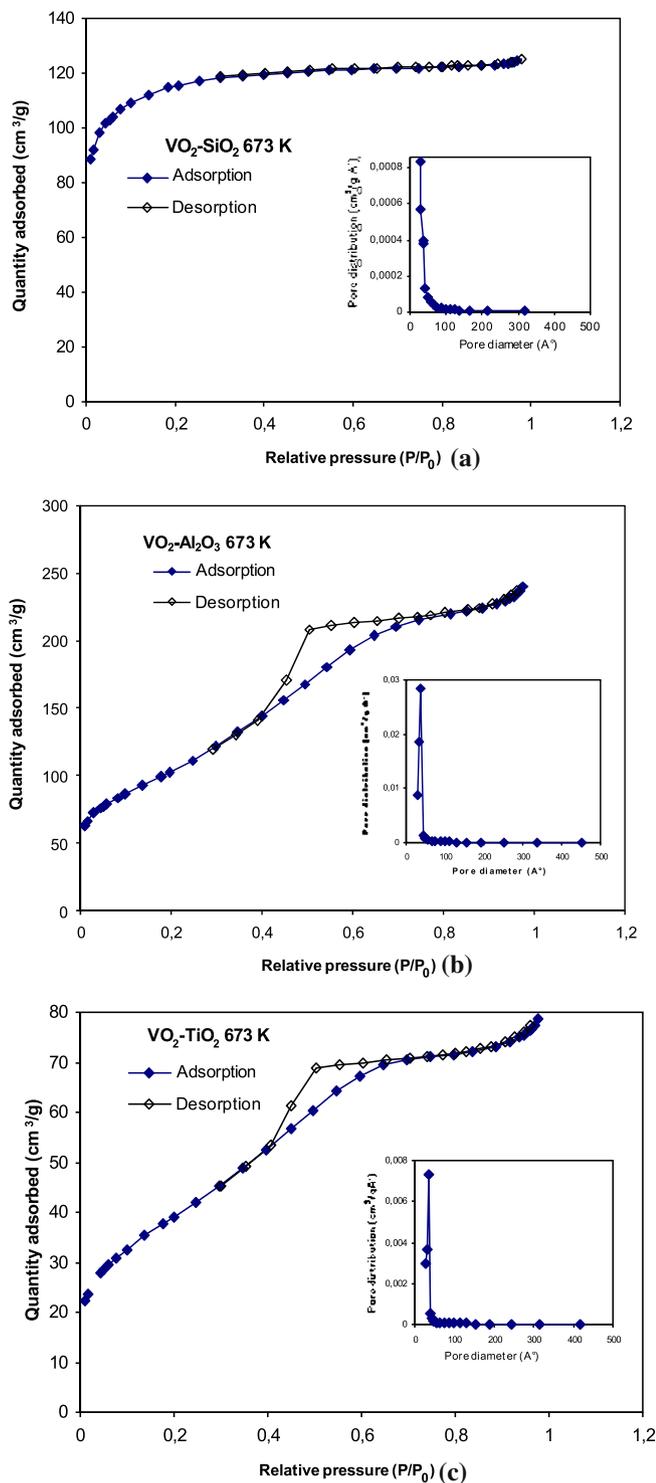
Figure 2. N_2 adsorption–desorption isotherms and pore size distribution of $5\%VO_2–M_xO_y$ samples: $VO_2–SiO_2$ (**a**), $VO_2–Al_2O_3$ (**b**) and $VO_2–TiO_2$ (**c**).

Figure 3. DR–UV-vis spectra of $5\%VO_2–M_xO_y$ materials: $VO_2–SiO_2$ (**a**), $VO_2–Al_2O_3$ (**b**) and $VO_2–TiO_2$ (**c**).

mesoporous structure. However, $VO_2–SiO_2$ isotherm can be classified as type-I with microporous structure.

The UV–Vis diffused reflectance spectra of $VO_2–Al_2O_3$, $VO_2–SiO_2$ and $VO_2–TiO_2$ are shown in figure 3. The absorption of $VO_2–Al_2O_3$ (673 K) in the range 250–400 nm can
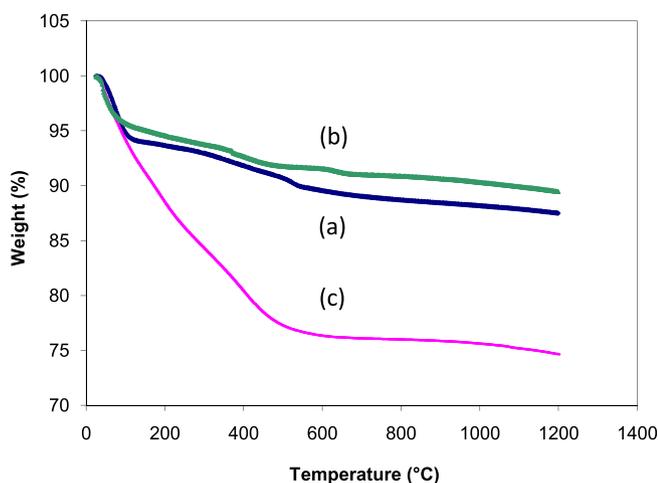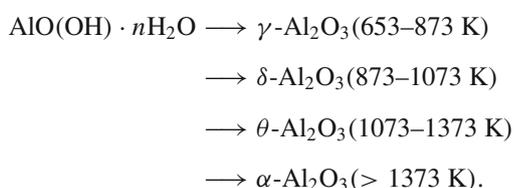
be considered negligible compared to that of $VO_2–Al_2O_3$ (1073 K) which displayed a wide and intense band at 350–450 nm. The observed band suggests a higher degree of condensation of vanadium oxide species (Aboelfetoh and Pietschnig 2009). The treatment at 1073 K caused a structural change of the material, making the vanadium sites to have better contact with common UV radiation (Bocuzzi *et al* 1998; Centeno *et al* 2002). This actually increased intensity of the spectrum and made appearance of the characteristic bands of VO_2 species between 350 and 450 nm (Li-Bin *et al* 2002). However, characteristic bands of alumina, 262 nm (Ivanova 2004) are masked by VO_2 species. Concerning the $VO_2–SiO_2$ samples (673 K and 1073 K),

UV-Vis spectra showed vanadium oxides adsorption bands in the range 350–450 nm. For titania, we detected four bands characteristic of anatase phase (Nur 2006); a band at 213 nm which corresponds to Ti^{4+} cations in a tetrahedral environment due to the electronic transition between Ti^{4+} and oxygen ligands (Zheng and Gao 2002; Cozzolino *et al* 2007), and the bands at 273, 312 and 333 nm characteristic of Ti^{4+} cations in an octahedral environment (Haskouri *et al* 2001; Cozzolino *et al* 2007). When vanadium was added to titania, a reduction in the spectrum intensity was observed. This was due to the deposition of vanadium oxides and was explained by the wide band between 450 and 350 nm. However, characteristic bands of Ti^{4+} species still existed, which affirmed the existence of two species TiO$_2$ and VO$_2$. The results of UV–Vis are confirmed by the results of XRD.

TGA curves of the thermally treated VO$_2$–SiO$_2$ (a) and VO$_2$–TiO$_2$ (b) in figure 4 show one weight loss step ($\sim$5 %) up to 423 K, which can be attributed to the removal of water trapped in the pores of the xerogel composite. TGA analysis also shows a continuous weight loss ($\sim$4–5%) up to 1273 K. According to earlier studies (Aboelfetoh and Pietschnig 2009), the weight loss between 573 and 1273 K can be attributed only to the loss of hydroxyl groups. In the case of VO$_2$–Al$_2$O$_3$ (c) in figure 4, an important continuous weight loss was observed up to 873 K which continues slowly up to 1273 K ($\sim$24 %) corresponding to the removal of water, surface hydroxyl groups and consequent transformation of boemithe to γ, δ and θ-alumina (Cruz and Eon 1998; Nguefack *et al* 2003).

$$AlO(OH) \cdot nH_2O \longrightarrow \gamma\text{-}Al_2O_3 (653\text{--}873 \text{ K})$$
$$\longrightarrow \delta\text{-}Al_2O_3 (873\text{--}1073 \text{ K})$$
$$\longrightarrow \theta\text{-}Al_2O_3 (1073\text{--}1373 \text{ K})$$
$$\longrightarrow \alpha\text{-}Al_2O_3 (> 1373 \text{ K}).$$

Figure 4. Thermogravimetric analysis of VO$_2$–SiO$_2$ (**a**), VO$_2$–TiO$_2$ (**b**) and VO$_2$–Al$_2$O$_3$ (**c**) samples before thermal treatment at 673 K.

Table 2. Amount of OH surface groups.

| Material	Weight loss (%)	OH groups (mmol/g material)
VO$_2$–Al$_2$O$_3$	8·16	4·80
VO$_2$–SiO$_2$	4·87	2·86
VO$_2$–TiO$_2$	3·40	2·00

Moreover, the amount of OH groups was estimated from TGA analysis. For this, the weight loss between 573 and 1273 K was determined (Aboelfetoh and Pietschnig 2009). The results are summarized in table 2. They show that OH surface groups on VO$_2$–Al$_2$O$_3$ are more than two times higher than those of silica and titania, even after thermal treatment.

SEM picture of the 5% VO$_2$–M$_x$O$_y$ materials after thermal treatment is shown in figure 5. For VO$_2$–SiO$_2$ (673 K), well-crystallized faceted grains are seen, with sizes of about 0·6 nm. They coexist with other larger grains. After treatment at 1073 K, a larger magnification with the same morphology can be obtained. Concerning VO$_2$–Al$_2$O$_3$ (673 K), small boehmite clusters of about 1·4 μm were bonded to each other. For VO$_2$–Al$_2$O$_3$ (1073 K), an agglomeration of small piles of grains, in the form of sponge ($\sim$9 μm), was seen. XRD showed that these are δ-Al$_2$O$_3$, corundum and VO$_2$. The presence of crystallized particles of $\sim$20 μm geometric shapes was observed in the case of VO$_2$–TiO$_2$ (673 K). This corresponds to the anatase.

The values of the surface atomic V, Ti, Si and Al concentrations from EDX analysis of the solids studied are shown in table 3. The surface V/Ti, V/Al and V/Si atomic ratios were very similar to the theoretical ones in the samples with a 5 wt.% V.

3.2 Catalytic activity results

The oxidation of cyclohexene with TBHP in the presence of vanadium mixed oxides resulted in the formation of several products as shown in table 4. Generally, cyclohexene oxidation yielded mainly cyclohexene oxide (epoxide) and cyclohexane diols, besides cyclohexenol (enol), cyclohexenone (enone), cyclohexanol (ol) and cyclohexanone (one). Through GC analysis, 1,2-cyclohexanediol was not detected in the reaction product (Jiang *et al* 2009). Cyclohexene conversion and epoxide selectivity varied significantly with catalyst composition. High cyclohexene conversion (21%) and epoxide selectivity ($\sim$84%) were observed in the case of VO$_2$–SiO$_2$ at 643 K. It is apparent that VO$_2$–SiO$_2$ at 643 K exhibits highest conversion. This may suggest that BET surface areas of the catalysts would play a more important role because BET surface areas of VO$_2$–SiO$_2$ at 643 K (390 m^2/g) is much bigger than those of VO$_2$–Al$_2$O$_3$ (368 m^2/g) and VO$_2$–TiO$_2$ (140 m^2/g) at 643 K (Mi *et al* 2009). As shown in table 4, VO$_2$–SiO$_2$ at 643 K exhibited
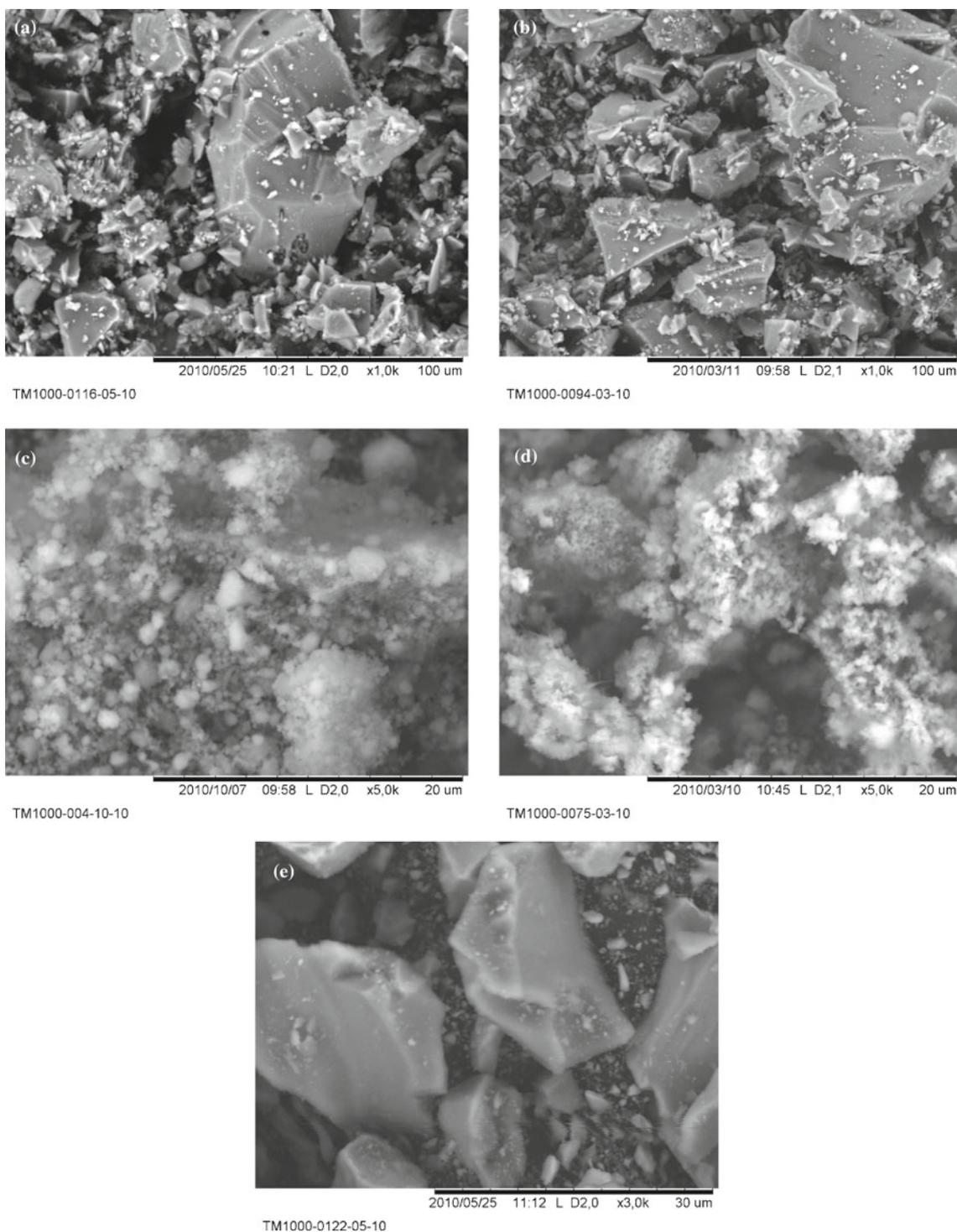
Figure 5. SEM photographs of 5%VO$_2$–M$_x$O$_y$ samples: VO$_2$–SiO$_2$ (673 K) (**a**), VO$_2$–SiO$_2$ (1073 K) (**b**), VO$_2$–Al$_2$O$_3$ (673 K) (**c**), VO$_2$–Al$_2$O$_3$ (1073 K) (**d**) and VO$_2$–TiO$_2$ (673 K) (**e**).

Table 3. EDX results of different materials.

Material	Weight (%)	Weight of V (%)
VO$_2$–Al$_2$O$_3$	84·8 (Al)	15·2
VO$_2$–SiO$_2$	89·2 (Si)	10·8
VO$_2$–TiO$_2$	92·7 (Ti)	7·3

highest selectivity to epoxide and VO$_2$–Al$_2$O$_3$ showed highest selectivity to cyclohex-2-en-1-ol. This may be due to the pore size of the catalysts. However, VO$_2$–SiO$_2$ at 643 K has a microporous structure (20 Å) but VO$_2$–Al$_2$O$_3$ and VO$_2$–TiO$_2$ has a mesoporous structure (40 and 35 Å).

The thermal treatment of VO$_2$–SiO$_2$ from 643 K to 1043 K, under argon, affected the conversion of cyclohexene,

Table 4. Oxidation of cyclohexene using different catalysts.

Catalysts	Conversion (%)		Selectivity (%)					
	TBHP	Cyclohexene	Epoxide	Enone	One	Enol	Ol	Diol
VO_2–SiO_2 (643 K)	24	21	83·51	–	12·72	3·78	–	–
VO_2–SiO_2 (1073 K)	20	13·49	68·14	18·3	8·56	–	–	–
VO_2–Al_2O_3 (643 K)	17	17·75	–	–	–	87·92	12·08	–
VO_2–Al_2O_3 (1073 K)	99	18·43	–	6·95	84·78	–	8·27	–
VO_2–TiO_2 (643 K)	57	13	21·45	15·9	20·49	42·16	–	–

(29 mmol C_6H_{12}; 38·45 mmol TBHP; 25 mL Heptane; 0·1 g catalyst; 6 h; 338 K)

where it decreased from 21% to 13·5%. That was due to a decrease of the surface area. However, it is still selective towards epoxide. In the case of VO_2–Al_2O_3, thermal treatment does not affect the conversion of cyclohexene due to the increase in pore size that reaches 196 Å despite the strong decrease in surface area. In this case, heat treatment promotes the formation of cyclohexanone.

4. Conclusions

5 wt.%Vanadia–silica, alumina or titania systems were prepared by inorganic precursors via the sol–gel process. The materials were calcined and reduced at 673 K and thermally treated under argon at 1073 K.

(I)   Results of XRD and DR UV-visible diffused revealed that VO_2 species were predominant in all samples and formation of V_2O_5 was not detected.

(II)   All samples showed a decrease of BET surface area with the increase of calcination temperatures due to sintering of the sample at higher calcination temperatures. VO_2–SiO_2 presented the highest surface area (390 m^2/g at 673 K).

(III) XRD patterns showed amorphous phase for VO_2–SiO_2 samples; however, VO_2–Al_2O_3 (673 K) presented only the characteristic peaks of the Al_2O_3 with boehmite phase $(AlO(OH)_nH_2O)$ and typical peaks of δ-Al_2O_3 and corundum and VO_2 crystalline at 1073 K. Concerning VO_2–TiO_2, the presence of TiO_2 anatase was detected as the only crystalline phase.

(IV) UV-Vis spectra of the considered solids confirmed the presence of VO_2.

(V)   TGA analysis showed a weight loss step for all samples, attributed to the removal of water trapped in the pores of the xerogel composite (up to 423 K) and to the loss of hydroxyl groups (up to 1473 K).

(VI) EDX results verified the percentage weight of vanadium in the catalysts.

(VII) The catalytic test of the epoxidation reaction of cyclohexene with hydroperoxide tert-butyl as oxidant, in the presence of different catalysts, showed that VO_2–SiO_2 directs the reaction towards epoxidation; however, VO_2–Al_2O_3 directs it towards the allylic oxidation.

References

Aboelfetoh E F and Pietschnig R 2009 *Catal. Lett.* **127** 83

Bellifa A, Lahcene D, Technar Y N, Choukchou-Braham A, Bachir R, Bedrane S and Kappenstein C 2006 *Appl. Catal. A: Gen.* **305** 1

Bocuzzi G C, Pinna F and Strukul G 1998 *J. Phys. Chem.* **B102** 5733

Bond G C and Tahir S F 1991 *Appl. Catal.* **71** 1

Brinker C J and Schere G W 1990 *Sol–gel science* (London: Academic Press)

Centeno M P, Montes M and Odriozola J A 2002 *Appl. Catal A: Gen.* **234** 65

Cozzolino M, Di Serio M, Tesser R and Santacesaria E 2007 *Appl. Catal. A: Gen.* **325** 256

Cruz A M and Eon J G 1998 *Appl.Catal. A: Gen.* **167** 203

Deo G, Wachs I E and Haber J 1994 *Crit. Rev. Surf. Chem.* **4** 14

Ertl G, Knozinger H and Weitkamp J (eds) 1997 *Handbook of heterogeneous catalysis* (Weinheim: Wiley-VCH)

Farrusseng D, Schlichte K, Spliethoff B, Wingen A, Kaskel S, Bradley J S and Schüth F 2001 *Angew. Chem. Int. Ed.* **40** 4204

Gregg S J and Sing K S W 1982 *Adsorption. Surface area and porosity* (London: Academic Press) 2nd ed

Habel D *et al* 2006 *J. Eur. Ceram. Soc.* **26** 3287

Hagen J 1999 *Industrial catalysis* (Weinheim: Wiley-VCH)

Haskouri J, Cabrera A, Gutierrez M, Beltrán-Porter A, Beltrán-Porter D, Marcos M D and Amorós P 2001 *Chem. Commun.* **4** 309

Ivanova S 2004 Etude de la réactivité d'agrégats métalliques de taille inférieure à 4 nm en atmosphère gazeuse soit oxydante soit réductrice. Doctorat these, University of Strasbourg, France

Jiang J, Ma K, Zhen Y, Cai S, Li R and Ma J 2009 *Catal. Lett.* **131** 105

Jiang X and Chen X 2004 *J. Catal.* **270** 547

Klein S, Thorimbert S and Maer W F 1996 *J. Catal.* **163** 476

Li-Bin L, Tie-Cheng L, Yong L and Qiang L 2002 *Nucl. Instrum. Meth. Phys. Res.* **B191** 102

Mi Y, Yang Z, Liu Z, Yang F, Sun Q, Tao H, Wang W and Wang J 2009 *Catal. Lett.* **129** 499

Miller J B and Ko E I 1997 *Catal. Today* **35** 269

Moussa N, Fraile J M, Ghorbel A and Mayoral J A 2006 *J. Mol. Catal A: Chem.* **255** 62

Nguefack M, Popa A F, Rossignol S and Kappenstein C 2003 *Phys. Chem. Chem. Phys.* **5** 4279

Nur H 2006 *Mater. Sci. Eng.* **B133** 49

Reddy B M, Khan A, Yamada Y, Kobayashi T, Loridant S and Volta J C 2002 *J. Phys. Chem.* **B106** 10964

Reddy B M, Khan A, Yamada Y, Kobayashi T, Loridant S and Volta J C 2003 *J. Phys. Chem.* **B107** 11475

Reddy B M, Rao K N, Reddy G K and Bharali P 2006 *J. Mol. Catal. A: Chem.* **253** 44

Sen T, Rajamohanan P R, Ganapathy S and Sivasanker S 1996 *J. Catal.* **163** 354

Sing K S J, Everett D H, Haul R A W, Moscou L, Pierotti R A, Rouquerol J and Siemieniewska T 1985 *Pure Appl. Chem.* **57** 603

Sreethawong T, Yamad Y, Kobayashi T and Yoshikawa S 2005 *J. Mol. Catal. A: Chem.* **241** 23

Technical Data Sheet 1997 Chemical Divisions, BASF Corporation

Thomas J M and Thomas W J 1997 *Heterogeneous catalysis* (Weinheim: VCH)

Weckhuysen B M and Keller D E 2003 *Catal. Today* **78** 25

Whitting B I and Anderson J R 1993 *J. Phys. Chem.* **97** 1032

Yejun G and Can L 2007 *Chinese J. Catal.* **28** 392

Yoldas B E 1975 *Am. Ceram. Soc. Bull.* **54** 289

Zheng S and Gao L 2002 *Mater. Chem. Phys.* **78** 512